· Article · Advances in Polar Science
doi: 10.13679/j.advps.2021.0053 September 2022 Vol. 33 No. 3: 244-252

Spatial variability of $\delta^{18}O$ and $\delta^{2}H$ in North Pacific and Arctic Oceans surface seawater

LI Zhiqiang[1], DING Minghu[2,3], WANG Yetang[4*], DU Zhiheng[3] & DOU Tingfeng[5]

[1] National Marine Environmental Forecasting Center, Beijing 100081, China;
[2] State Key Laboratory of Severe Weather and Institute of Tibetan Plateau & Polar Meteorology, Chinese Academy of Meteorological Sciences, Beijing 100081, China;
[3] State Key Laboratory of Cryospheric Science, Northwest Institute of Eco-Environment and Resources, Chinese Academy of Sciences, Lanzhou 730000, China;
[4] College of Geography and Environment, Shandong Normal University, Jinan 250014, China;
[5] College of Resources and Environment, University of Chinese Academy of Sciences, Beijing 100049, China

Received 16 November 2021; accepted 22 August 2022; published online 30 September 2022

Abstract This study presents new observations of stable isotopic composition ($\delta^{18}O$, $\delta^{2}H$ and deuterium excess) in surface waters of the North Pacific and Arctic Oceans that were collected during the sixth Chinese National Arctic Research Expedition (CHINARE) from mid-summer to early autumn 2014. Seawater $\delta^{18}O$ and $\delta^{2}H$ decrease with increasing latitudes from 39°N to 75°N, likely a result of spatial variability in evaporation/precipitation processes. This explanation is further confirmed by comparing the $\delta^{18}O$–$\delta^{2}H$ relationship of seawater with that of precipitation. However, effects of freshwater inputs on seawater stable isotopic composition are also identified at 30°N–39°N. Furthermore, we find a non-significant relationship between the isotopic parameters ($\delta^{2}H$ and $\delta^{18}O$) and salinity from 73°N northwards in the Arctic Ocean, implying that sea ice melting/formation may have some effect. These results suggest that the isotopic parameters $\delta^{2}H$ and $\delta^{18}O$ are useful for tracing marine hydrological processes.

Keywords **stable water isotopes**, **seawater salinity**, **surface seawater**, **North Pacific Ocean**, **Arctic Ocean**

Citation: Li Z Q, Ding M H, Wang Y T, et al. Spatial variability of $\delta^{18}O$ and $\delta^{2}H$ in North Pacific and Arctic Oceans surface seawater. Adv Polar Sci, 2022, 33(3): 244-252, doi: 10.13679/j.advps.2021.0053

1 Introduction

The isotopic ratios of seawater $\delta^{18}O$ and $\delta^{2}H$, which represent the isotopic abundance ratios of $^{18}O/^{16}O$ and $^{2}H/^{1}H$, respectively, in a sample with respect to those of Vienna Standard Mean Ocean Water (VSMOW) are associated with fractionation processes that occur during all phase transitions in the hydrological cycle, including evaporation, precipitation, melting, and freezing of freshwater in the ocean. Thus, in modern oceans, seawater isotopes can serve as valuable natural tracers of sea ice melt (Macdonald et al., 1999), the source(s) of freshwater input (Khatiwala et al., 1999; Dubinina et al., 2017), and the formation of deep ocean water (Jacobs et al., 1985). They have also been used to trace the flow pathways of freshwater to the sea and to quantify the exchanges between different water masses (Gordeev et al., 1996; Bauch et al., 2005; Dubinina et al., 2017). Furthermore, the seawater stable isotopes of hydrogen and oxygen are considered

* Corresponding author, ORCID: 0000-0003-2499-1147, E-mail: wangyetang@163.com

important proxies for reconstructing palaeoclimate (Craig and Gordon, 1965; Sowers and Bender, 1995; Koutavas and Joanides, 2012) and palaeosalinity, an important parameter for understanding the ocean hydrological cycle (Rohling and Bigg, 1998; Singh et al., 2014).

Several previous studies have documented that seawater $\delta^{18}O$, δD, and their relationship can be used to understand oceanic hydrological processes (Conroy et al., 2014; Dubinina et al., 2017; Kumar et al., 2018). To quantify ocean isotopic signatures, many seawater $\delta^{18}O$ measurements have been made across the world's oceans from 1950 onwards (LeGrande and Schmidt, 2006). However, such observations over the North Pacific Ocean and the Arctic Ocean remain limited, and so oceanic hydrological processes remain inadequately characterized. Thus, additional seawater isotope observations are still required.

Deuterium excess (d), defined as $d=\delta^{2}H-8\times\delta^{18}O$ (Dansgaard, 1964), quantifies non-equilibrium fractionation effects during phase changes. This second-order parameter depends largely on the conditions, such as relative humidity, sea surface temperature (SST), and wind speed, in the region of moisture origin, i.e., where water evaporates from the ocean surface (Dansgaard, 1964; Pang et al., 2015; Parkes et al., 2017). Thus, ocean surface conditions have a strong impact on d values in vapor or subsequent precipitation (Uemura et al., 2008). As a result, changes in surface seawater d values likely affect the d variations measured in vapor and precipitation. Many efforts have been made to investigate the spatial and temporal variability vapor and precipitation d values, and to infer their main underlying processes (Aemisegger et al., 2014; Benetti et al., 2014; Pfahl and Sodemann, 2014). However, data on the spatial variability of seawater d values and inferences regarding their underlying mechanisms are still somewhat limited.

Here, we present new isotope data of surface seawater collected along the route of the sixth Chinese National Arctic Research Expedition (CHINARE), which took place from July to September 2014 (Figure 1). Based on this dataset, we investigate the spatial patterns in seawater stable isotopic compositions, quantify $\delta^{2}H$–$\delta^{18}O$ relationships, and analyze their possible controlling factors.

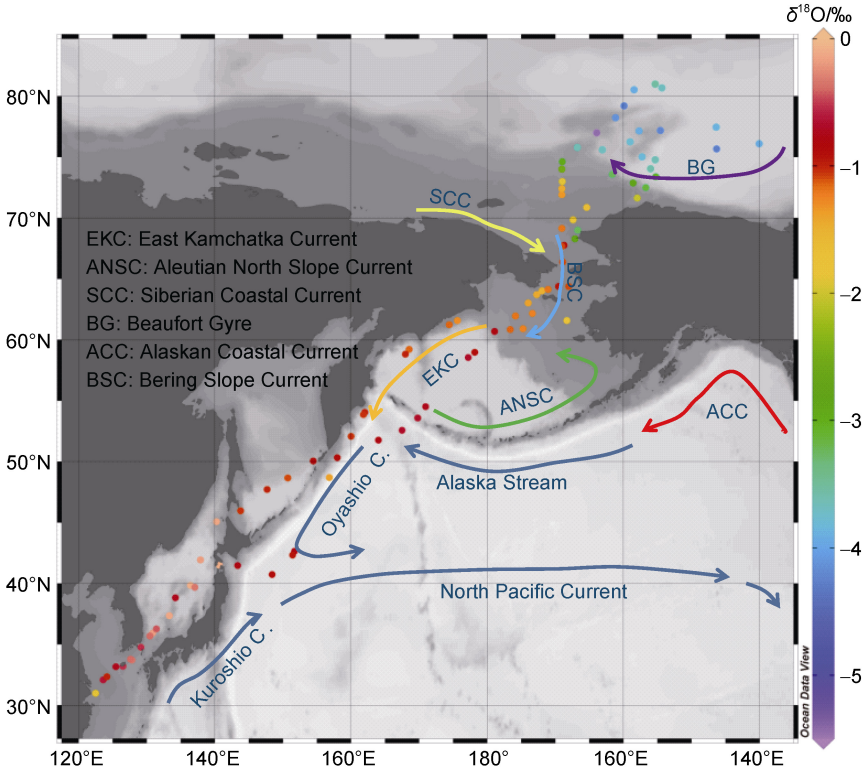

Figure 1 The route of the 6th CHINARE and the locations of the seawater isotopic composition and surface salinity samplings.

2 Data and methods

During the 6th CHINARE cruise (July to September of 2014), sea surface water samples were collected every 12 h along the route shown in Figure 1. The route spans the East China Sea, the Japan Sea, the Northwest Pacific Ocean, the Bering Sea, the Chukchi Sea, and the Arctic Ocean. The northern-most sampling location was at 81°N, 155°E. In total, 178 250-mL high-density polyethylene (HDPE) bottles were used to collect surface water. To prevent contamination, a 10-L bucket was used to collect surface water and first wash and then fill the bottles at each site. Then, the tightly capped bottles were placed into separate Ziploc bags and were refrigerated. Two bottles of seawater

were sampled at each location to determine whether sample contamination may have occurred.

Stable water isotopic compositions were measured at the State Key Laboratory of Cryospheric Sciences, China by wavelength scanned cavity ring-down spectrometry (CRDS) (Picarro L1102), with an overall precision of at least 0.15‰ for δ^{18}O and 0.5‰ for δ^{2}H. Using the isotope ratio mass spectrometry (IRMS) method, salinity correction to δ values was considered unnecessary because the molalities of Mg, Ca, and K were lower than the values used for correction (Gonfiantini, 1981). As a modern method, near-infrared laser absorption spectroscopy techniques (including CRDS) have also proven applicable to seawater experiments (Skrzypek and Ford, 2014). The main effect (incomplete evaporation and memory effect) of salinity is related to the vaporizer. Thus, the in-time replacement of the injection pad per 100 injections of seawater samples was applied in our measurements. Isotopic compositions are reported as δ^{18}O and δ^{2}H values and represent the differences in the ^{18}O/^{16}O and D/H ratios, respectively, between the samples and VSMOW.

Based on results from four world-class laboratories (Benetti et al., 2017), when applying the CRDS method to sea-water, and additional correction of ~0.09‰ is required for δ^{18}O compared with freshwater. This is slightly larger than that the IRMS method requires (0.06‰–0.02‰). However, for δ^{2}H, only ~0.13‰ of extra correction is required, which is much less than that required by IRMS measurements (0.55‰–0.23‰). Regardless, the errors of both methods were minimized by applying rigorous experimental protocols and conducting calibration.

Surface seawater was collected from an intake on the port side of the ship at approximately 4-m depth, which was designed to capture representative surface biogeochemical signals. To minimize clogging by sea ice and reduce the residence time of the sampling, a sea chest was specifically designed (details can be found in Chen et al. (2015)). We measured the SST and salinity continuously along the cruise route by means of an SBE21 (Sea-Bird Electronics) thermosalinograph installed in the sea chest, which has been widely used for observational marine chemistry studies.

All instruments were calibrated and tested before deployment. Instrumental uncertainty in the temperature and conductivity sensors was 0.002℃ and ~0.03 ms · cm^{-1}, respectively. Salinities given by the conductivity sensors are in practical salinity units (PSU). This information was also introduced by He et al. (2015), Chen et al. (2015) and Chen et al. (2019).

3 Results and discussion

3.1 Spatial patterns if δ^{18}O and δ^{2}H in surface seawater

Along the voyage route northwards, seawater δ^{2}H varies from −50.0‰ to −0.6‰, and the range of δ^{18}O values is between −5.4‰ and −0.1‰. Both the δ^{18}O and δ^{2}H values of surface seawater vary spatially as a function of latitude. As expected, they decrease with increasing latitude, with the heavy isotopes being relatively enriched in the mid-latitudes and depleted in the high-latitude Arctic Ocean (Figures 1 and 2). This finding agrees with the observed changes in meteoric water due to latitudinal temperature and precipitation effects (Craig and Gordon, 1965; Criss, 1999). Latitude is also an important factor affecting spatial changes in *d*, but only for the sampling sites at <40° latitude and >70° latitude (Figure 2). About 25% and 40% of the spatial variance of *d* can be explained by the linear regression models, respectively.

However, from 30°N to 39°N, the seawater δ^{18}O and δ^{2}H values show increases of 0.1‰ and 0.6‰, respectively, per degree of latitude. Salinity values follow the δ^{18}O and δ^{2}H patterns, but a slight decrease in the SST is observed. In particular, extremely low salinity: δ^{18}O ratios occur between 36°N and 45°N, and thus the increase in the δ^{18}O and δ^{2}H values may be associated with the input of surface runoff (freshwater). Given the extremely high correlation between δ^{18}O and δ^{2}H (r>0.98, p=0), we further investigated regional patterns in the stable isotopic composition in surface seawater using δ^{18}O. Between 40°N and 62°N, the SST sharply decreases from 20℃ to 5℃, whereas the salinity gradually decreases from 33.9 to 30.7 PSU. The corresponding δ^{18}O values vary by 1.7‰ (from −1.8‰ to −0.1‰). From 62°N to 77°N, the SST fluctuates from −0.7℃ to 10℃. In this latitudinal range, sharp changes in seawater salinity and δ^{18}O also occur, with decreases of 11 PSU and 4.5‰, respectively. From 77°N northwards, the seawater salinity is lower, but a slight increase in the seawater δ^{18}O is observed, which may be an effect of sea ice melt; sea ice usually has higher δ^{18}O values than the underlying seawater because relatively more ^{18}O is incorporated into ice than the water from which it froze. During the freezing or melting of seawater, the δ^{18}O values do not change much due to the small fractionation factor involved in the transition between ice and water (Beck and Münnich, 1988; Melling and Moore, 1995). In contrast, the influence of sea ice formation or melt on seawater salinity changes is large because of the extremely low salinity of sea ice (the salinity of sea ice is usually as low as 4 PSU; Ekwurzel et al., 2001). Our samples in the Arctic Ocean were collected between late July and early September of 2014, when sea ice extent is at or close to its annual minimum (Figure 3). Extensive sea ice melt led to a slight increase in seawater δ^{18}O and a decrease in salinity.

To further determine spatial patterns in the seawater stable isotopic composition, we identify different areas of the North Pacific and Arctic Oceans via a clustering analysis (Clusters 1–5 in Figure 4). Analysis of variance (ANOVA) was used to test the statistical significance of the differences between the clusters. Here, we use the 0.05 significance level. Cluster 1 samples are from the East

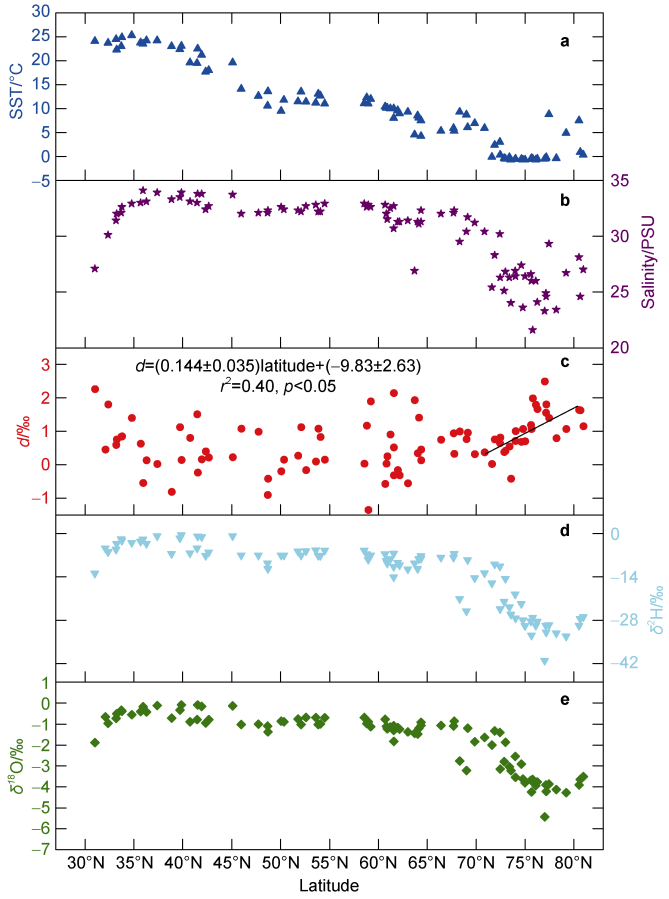

Figure 2 Latitudinal distributions of SST (**a**), salinity (**b**), deuterium excess (*d*) (**c**), $\delta^{2}H$ (**d**), and $\delta^{18}O$ (**e**) in surface ocean waters.

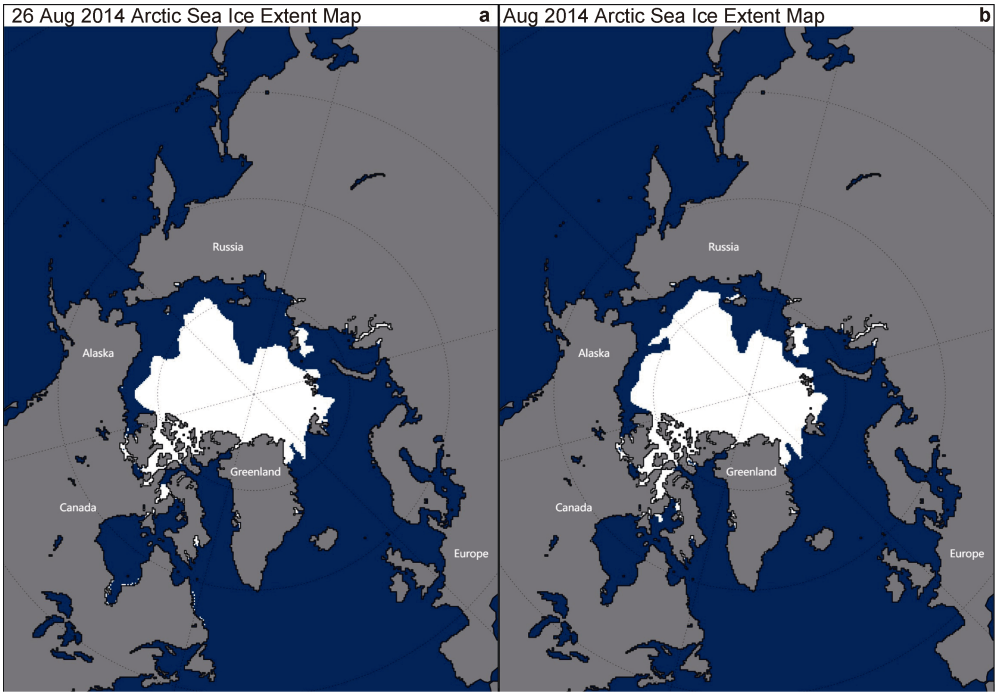

Figure 3 Arctic sea ice extent on 26th August 2014 (**a**) and monthly mean sea ice extent in August 2014 (**b**). Data are from NSIDC: https://nsidc.org/data/NSIDC-0051.

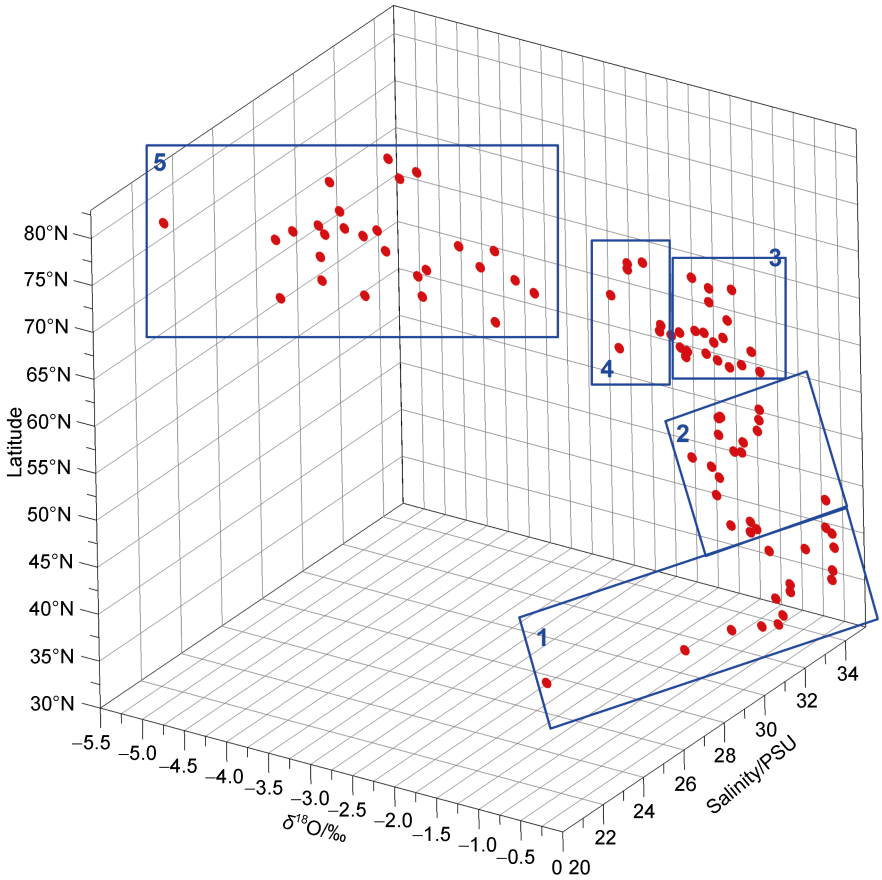

Figure 4 Three-dimensional plot showing $\delta^{18}O$ vs. salinity vs. latitude, which helps to identify the regional features of the seawater $\delta^{18}O$ and δ-salinity relationship.

China Sea and the Sea of Japan (30°N–40°N), where a large range of $\delta^{18}O$ values are observed and the SST decreases sharply with increasing latitude. $\delta^{18}O$ values and salinities in Cluster 2, which are from the region of the North Pacific Ocean, dominated by Kuroshio Current, are higher Clusters 3 and 4 were sampled over the region of the Bering Sea where there are three main currents; the Bering Slope Current, the Kamchatka Current, and the Aleutian North Slope Current (Stabeno et al., 1999). The $\delta^{18}O$ values range from −3.5‰ to −1‰, which broadly agree with those obtained in previous surface water samplings from Bering Sea (Cooper et al., 1997). Based on the linear regression of $\delta^{18}O$ with salinity by the least squares fit, the *y*-intercept of zero salinity for $\delta^{18}O$ is −11.1‰, which is similar to the mean $\delta^{18}O$ value of freshwater between meteoric water values and melted sea ice. Cooper et al. (1991) reported a freshwater $\delta^{18}O$ value of approximately −22‰ in the Yukon River, which is the largest river entering the Bering Sea. According to Macdonald et al. (1989, 1999), $\delta^{18}O$ values in the sea ice and sea ice melt range from −3‰ to −2‰. The mean $\delta^{18}O$ value of all sea ice collected during 2010 and 2011 in the Chukchi Sea were reported to be approximately −1‰ (Cooper et al., 2016). Cluster 5 (73°N to 81°N) was sampled from the Arctic Ocean and has lower $\delta^{18}O$ and salinities than the other clusters.

3.2 δD and $\delta^{18}O$ relationship in sea surface water

The pioneering work by Craig (1961) reported the quantitative relationship between $\delta^{2}H$ and $\delta^{18}O$ in precipitation, with $\delta^{2}H = 8\times\delta^{18}O+10$, which is known as the meteoric water line (MWL). This relationship has been explained physically by an isotopic fractionation Raleigh-type mode. The robust relationship between $\delta^{2}H$ and $\delta^{18}O$ was also observed in Antarctic surface snow by Masson-Delmotte et al. (2008). Given that the combined application of seawater $\delta^{2}H$ and $\delta^{18}O$ measurements can quantitatively improve paleohydrology and palaeosalinity reconstructions (Rohling, 2007; Holloway et al., 2016), increasing attention has been paid to the use of $\delta^{2}H$ for palaeosalinity reconstruction (e.g., Roberts et al., 2016). However, the seawater $\delta^{2}H$–$\delta^{18}O$ relationship is still not well documented. Our observations show a high and significant correlation between $\delta^{2}H$ and $\delta^{18}O$ in seawater over the North Pacific and Arctic Oceans, with a slope of 7.7‰±0.1‰ per ‰ (r>0.99, p<0.01), which is close to both the global average seawater $\delta^{2}H$–$\delta^{18}O$ slope of 7.4 (Rohling, 2007) and the slope of the global MWL derived from Global Network of Isotopes in Precipitation (GNIP) precipitation data (Rozanski et al., 1993). For the distinct regions in the North Pacific and Arctic Oceans identified by

clustering (as described above), strong correlations between $\delta^{2}H$ and $\delta^{18}O$ in seawater were found for all clusters, despite the differences in their gradients (Figure 5). Cluster 1 had the shallowest seawater $\delta^{2}H$-$\delta^{18}O$ slope of 6.9‰ per ‰. This possibly reflects the impact of continental runoff, which generally has a lower $\delta^{2}H$-$\delta^{18}O$ slope than seawater (e.g., Deshpande et al., 2013). The steepest $\delta^{2}H$-$\delta^{18}O$ slope (7.8‰ per ‰) was observed in Clusters 3 and 4.

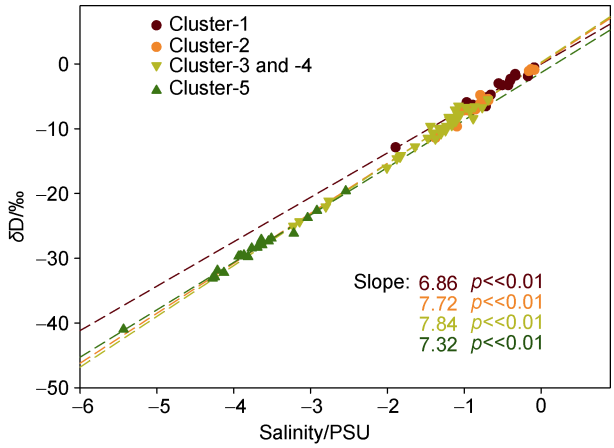

Figure 5 The relationship between seawater $\delta^{18}O$ and $\delta^{2}H$ for the different regions (clusters) of the North Pacific and Arctic Oceans. The dotted lines indicate the linear regressions on the data from the different clusters. *p* denotes the significance of the relationships according to the linear regression analysis.

3.3 Spatial variability in the *d* values of surface seawater

Along the 6th CHINARE route, seawater *d* values varied from −1.3‰ to 2.5‰. In the Arctic Ocean, a significant positive correlation between *d* and latitude was evident (r=0.63, p<0.05), but a significant negative correlation exists between seawater *d* and $\delta^{18}O$ (r=−0.68, p<0.05). Given that the spatial distributions of *d* and $\delta^{18}O$ are often used for model validation (Xu et al., 2012), the spatial distribution of *d* as a function of latitude that best fits the *d* spatial distribution (Figure 2) was calculated. However, no significant correlations between the seawater *d* values and latitude or $\delta^{18}O$ were found over the North Pacific Ocean (Figure 2).

Along the 6th CHINARE route from the Bering Strait to the interior of the Arctic Ocean (from 66°N northward), *d* values of surface seawater at all sampling sites (except one) are positive, suggesting the possibly of strong runoff impacts (Xu et al., 2012). The $\delta^{18}O$-salinity relationship for the sampling sites from 66°N to 70°N shows the *y*-intercept (salinity=0) of $\delta^{18}O$ is −24‰±6‰ (r^2=0.74, n=8), indicating the large freshwater contribution of river runoff into the Bering Strait. The *y*-intercept (salinity=0) $\delta^{18}O$ value from 71°N to 80°N is estimated to be −9.3‰±2.2‰ (r^2=0.23, n=27), which reflects a fraction of melted sea ice in the surface seawater. However, this contribution is most likely very limited for seawater along our cruise track because the heavy oxygen isotopes become substantially more depleted along the cruise route into the interior of the Arctic Ocean, with a $\delta^{18}O$ value as low as <−5‰ at ~77°N in the Beaufort Gyre. Our results over the Chukchi Sea are broadly consistent with previously reported surface seawater $\delta^{18}O$ value ranges (approximately −4‰ to approximately 1‰) (Cooper et al., 1997, 2016). Morison et al. (2012) revealed the insignificant role of melted sea ice in the freshwater of seawater in the Beaufort Gyre, where runoff from Siberian sources can be transported via Arctic Ocean surface water circulation.

3.4 Processes controlling spatial variability in the stable isotopic composition of surface seawater

The processes controlling variations in stable isotopes in seawater include evaporation, precipitation, sea ice freezing and melting, and advection and diffusion of water masses from different source regions. Figure 6 shows the

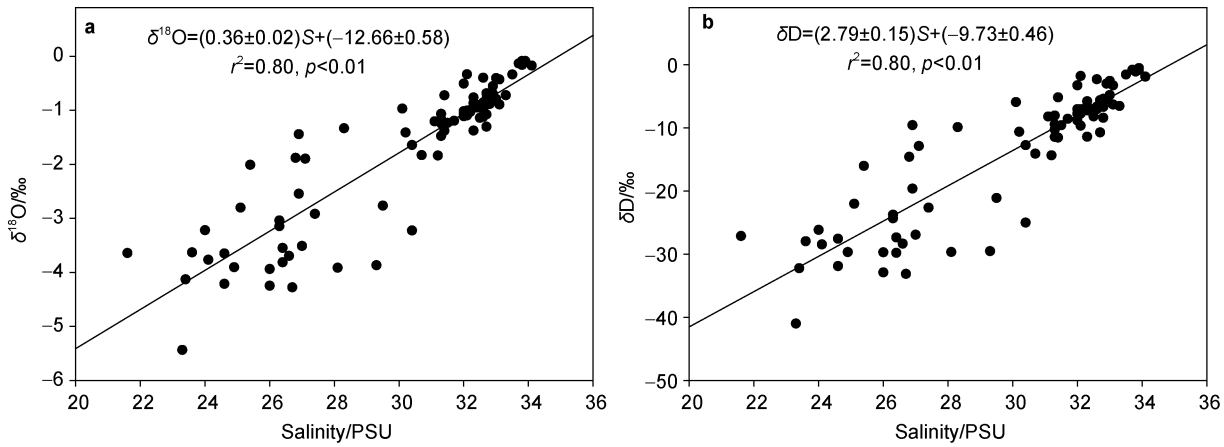

Figure 6 The relationships between surface sea salinity and seawater $\delta^{18}O$ (**a**), and surface sea salinity and seawater $\delta^{2}H$ (**b**) from the North Pacific and Arctic Oceans.

quantitative relationship between $\delta^{18}O$, $\delta^{2}H$, and salinity in seawater along the voyage route. A robust positive correlation is observed along the whole route, with slopes of 0.4‰±0.02‰/PSU for $\delta^{18}O$ (n=90, p<0.01) and 2.8‰± 0.15‰/PSU for δD (n=90, p<0.01).

To explore the other processes affecting spatial changes in seawater stable isotopes, we analyzed the oxygen isotope-salinity ($\delta^{18}O$-S) relationships for the regional clusters (Figure 7). Cluster 1, which corresponds to the East China Sea and the Sea of Japan, exhibits a shallow slope of 0.2‰/PSU, which is broadly consistent with those previously reported for the Tsushima Strait (0.2‰/PSU) and the Tsushima Current in the Sea of Japan (0.3‰/PSU) (Kodaira et al., 2016). In the East China Sea and the Tsushima Strait, diluted water from Changjiang is the main driver of low salinity and $\delta^{18}O$ values (Zhang et al., 1990; Kodaira et al., 2016). For the Tsushima Current, terrestrial water inputs from the Japanese Archipelago are responsible for the low salinity and $\delta^{18}O$ values (Kodaira et al., 2016). Thus, surface runoff likely plays an important role in the $\delta^{18}O$ changes for Cluster 1. Cluster 2 has the steepest $\delta^{18}O$-S slope of 0.6‰/PSU (Figure 7), which seems to suggest that the seawater composition of this area may be predominantly controlled by evaporation/precipitation. There was no statistically significant difference in the $\delta^{18}O$-S slope between Clusters 3, 4, and 1 (p>0.05). The data for Cluster 5 indicate a $\delta^{18}O$-S slope of 0.11‰/PSU (r^2=0.09), but the relationship is not statistically significant (p=0.16). This implies that sea ice melting/freezing has an important impact on the $\delta^{18}O$ and salinity values in this region. Sea ice formation/melting has large effects on seawater salinity. However, its impact on the isotopic composition in seawater is minor because of the small fractionation between sea ice and seawater. Thus, a large range of salinities rather than large changes in $\delta^{18}O$ values are observed in the surface ocean where sea ice formation and melting occur. Furthermore, the seasonality of sea ice extent also results in seasonal changes in the δ-salinity relationship. Over the Arctic Ocean, the maximum sea ice extent generally occurs in March, and the minimum in September (Figure 4), when our sampling took place. The δ-salinity slopes in September may be larger than those in other seasons due to the reduction in the salinity of surface seawater caused by extensive sea ice melting in this season.

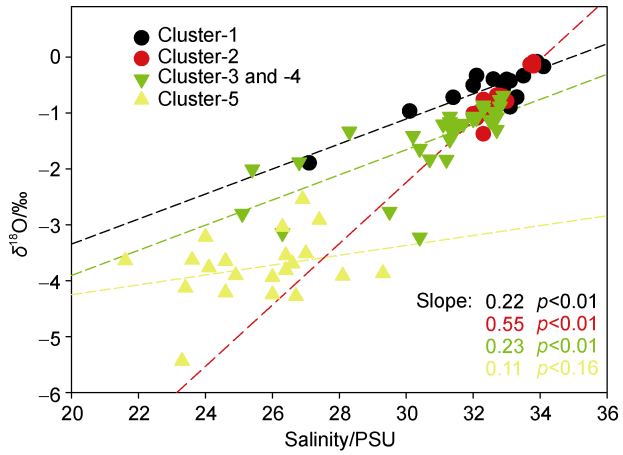

Figure 7 The relationship between seawater $\delta^{18}O$ and salinity for the different sections of the North Pacific and Arctic Oceans according to the clusters shown in Figure 4.

4 Conclusions

In this study, we present new measurements of the stable isotopic composition of surface seawater along the routes of the 6th CHINARE voyage. This campaign has helped to improve the coverage of isotopic measurements in the North Pacific and Arctic Oceans. SST and salinity were also measured. This new dataset allows us to examine the spatial variation in the stable isotopic composition, the $\delta^{18}O$-$\delta^{2}H$ relationship, and the $\delta^{18}O$-salinity relationship, and hence helps trace hydrological processes.

A strong $\delta^{18}O$-$\delta^{2}H$ relationship was found, which makes it possible to extrapolate seawater $\delta^{2}H$ based on $\delta^{18}O$. Seawater $\delta^{18}O$ and $\delta^{2}H$ values exhibit latitudinal changes, with decreasing values as latitude increases. The robust correlation between seawater $\delta^{18}O$ and $\delta^{2}H$ and salinity across the North Pacific and Arctic Oceans suggest that spatial pattern may largely result from evaporation/ precipitation effects. However, north of 73°N, sea ice melting plays a key role in the $\delta^{18}O$, $\delta^{2}H$, and salinity changes. This finding can be further confirmed because a significant correlation between d and latitude is present over the Arctic Ocean but not over the North Pacific Ocean. The lack of significant correlation over the North Pacific may be associated with a decline in evaporation causing an increased sea ice extent with increased latitude, driving up d variations.

Our new dataset still represents only three months and is subject to the temporal biases inherent in most $\delta^{18}O$ and $\delta^{2}H$ data. In the future, seasonal and long-term observations of seawater stable isotopes are required to examine whether the $\delta^{18}O$-$\delta^{2}H$ relation varies over time. Furthermore, these data are important for studying the stability of the δ-salinity relationship over time (Delaygue et al., 2001; Kumar et al., 2018) because seawater isotopes are associated with varying origins and pathways of atmospheric vapor, whereas seawater salinity is not.

Acknowledgements This work was funded by the National Natural Science Foundation of China (Grant no. 41771064), the National Key Basic Research Program of China (Grant no. 2019YFC1509100), the Basic Research Fund of Chinese Academy of Meteorological Sciences (Grant no. 2021Z006), the Project for Outstanding Youth Innovation Team in the Universities of Shandong Province (Grant no. 2019KJH011), and the 6th CHINARE. We appreciate two anonymous reviewers, and Associate Editor, Dr. Cinzia Verde for their constructive comments that have further improved the manuscript.

References

Aemisegger F, Pfahl S, Sodemann H, et al. 2014. Deuterium excess as a proxy for continental moisture recycling and plant transpiration. Atmos Chem Phys, 14(8): 4029-4054, doi:10.5194/acp-14-4029-2014.

Bauch D, Erlenkeuser H, Andersen N. 2005. Water mass processes on Arctic shelves as revealed from $\delta^{18}O$ of H_2O. Glob Planet Change, 48(1-3): 165-174, doi:10.1016/j.gloplacha.2004.12.011.

Beck N, Münnich K O. 1988. Freezing of water: isotopic fractionation. Chem Geol, 70(1-2): 168, doi:10.1016/0009-2541(88)90693-6.

Benetti M, Sveinbjörnsdóttir A E, Ólafsdóttir R, et al. 2017. Inter-comparison of salt effect correction for $\delta^{18}O$ and $\delta^{2}H$ measurements in seawater by CRDS and IRMS using the gas-H_2O equilibration method. Mar Chem, 194: 114-123, doi:10.1016/j.marchem.2017.05.010.

Benetti M, Reverdin G, Pierre C, et al. 2014. Deuterium excess in marine water vapor: dependency on relative humidity and surface wind speed during evaporation. J Geophys Res Atmos, 119(2): 584-593, doi:10.1002/2013jd020535.

Chen B, Cai W, Chen L. 2015. The marine carbonate system of the Arctic Ocean: Assessment of internal consistency and sampling considerations, summer 2010. Mar Chem, 176: 174-188, doi: 10.1016/j.marchem.2015.09.007.

Chen Z K, Wei L X, Li Z Q, et al. 2019. Sea fog characteristics over the Arctic pack ice in summer 2017. Mar Forecasts, 36(2): 77-87, doi:10.11737/j.issn.1003-0239.2019.02.009 (in Chinese with English abstract).

Conroy J L, Cobb K M, Lynch-Stieglitz J, et al. 2014. Constraints on the salinity-oxygen isotope relationship in the central tropical Pacific Ocean. Mar Chem, 161: 26-33, doi:10.1016/j.marchem.2014.02.001.

Craig H. 1961. Isotopic variations in meteoric waters. Science, 133(3465): 1702-1703, doi:10.1126/science.133.3465.1702.

Craig H, Gordon L I. 1965. Deuterium and oxygen 18 variations in the ocean and the marine atmosphere//Tongiorgi E (Eds). Stable isotopes in oceanographic studies and paleotemperatures. Spoleto: Cons Naz di Rech, 9-130.

Criss R E. 1999. Principles of stable isotope distribution. New York: Oxford University Press.

Cooper L W, Olsen C R, Solomon D K, et al. 1991. Stable isotopes of oxygen and natural and fallout radionuclides used for tracing runoff during snowmelt in an Arctic watershed. Water Resour Res, 27(9): 2171-2179, doi:10.1029/91wr01243.

Cooper L W, Whitledge T E, Grebmeier J M, et al. 1997. The nutrient, salinity, and stable oxygen isotope composition of Bering and Chukchi Seas waters in and near the Bering Strait. J Geophys Res Ocean, 102(C6): 12563-12573, doi:10.1029/97jc00015.

Cooper L W, Frey K E, Logvinova C, et al. 2016. Variations in the proportions of melted sea ice and runoff in surface waters of the Chukchi Sea: a retrospective analysis, 1990–2012, and analysis of the implications of melted sea ice in an under-ice bloom. Deep Sea Res Part II Top Stud Oceanogr, 130: 6-13, doi:10.1016/j.dsr2.2016.04.014.

Dansgaard W. 1964. Stable isotopes in precipitation. Tellus, 16(4): 436-468, doi:10.3402/tellusa.v16i4.8993.

Delaygue G, Bard E, Rollion C, et al. 2001. Oxygen isotope/salinity relationship in the northern Indian Ocean. J Geophys Res Oceans, 106(C3): 4565-4574, doi:10.1029/1999jc000061.

Deshpande R D, Muraleedharan P M, Singh R L, et al. 2013. Spatio-temporal distributions of $\delta^{18}O$, δD and salinity in the Arabian Sea: identifying processes and controls. Mar Chem, 157: 144-161, doi:10.1016/j.marchem.2013.10.001.

Dubinina E O, Kossova S A, Miroshnikov A Y, et al. 2017. Isotope (δD, $\delta^{18}O$) systematics in waters of the Russian Arctic seas. Geochem Int, 55(11): 1022-1032, doi:10.1134/S0016702917110052.

Ekwurzel B, Schlosser P, Mortlock R A, et al. 2001. River runoff, sea ice meltwater, and Pacific water distribution and mean residence times in the Arctic Ocean. J Geophys Res, 106(C5): 9075-9092, doi:10.1029/1999jc000024.

Gonfiantini R. 1981. The δ-notation and the mass-spectrometric measurement techniques//Gat J R, Gonfiantini R (Eds). Stable isotope hydrology: deuterium and oxygen-18 in the water cycle. Tech Rep Ser 210. Vienna: International Atomic Energy Agency, 337.

Gordeev V V, Martin J M, Sidorov I S, et al. 1996. A reassessment of the Eurasian river input of water, sediment, major elements, and nutrients to the Arctic Ocean. Am J Sci, 296(6): 664-691, doi:10.2475/ajs.296.6.664.

He Y, Liu N, Chen H X, et al. 2015. Observed features of temperature, salinity and current in central Chukchi Sea during the summer of 2012. Acta Oceanol Sin, 34(5): 51-59, doi:10.1007/s13131-015-0642-7.

Holloway M D, Sime L C, Singarayer J S, et al. 2016. Reconstructing paleosalinity from $\delta^{18}O$: Coupled model simulations of the Last Glacial Maximum, Last Interglacial and Late Holocene. Quat Sci Rev, 131: 350-364, doi:10.1016/j.quascirev.2015.07.007.

Jacobs S S, Fairbanks R G, Horibe Y. 1985. Origin and evolution of water masses near the Antarctic continental margin: evidence from $H_2{}^{18}O/H_2{}^{16}O$ ratios in seawater//Jacobs S S. Oceanology of the Antarctic Continental Shelf, Volume 43. Washington D. C.: American Geophysical Union, 59-85, doi:10.1029/ar043p0059.

Khatiwala S P, Fairbanks R G, Houghton R W. 1999. Freshwater sources to the coastal ocean off northeastern North America: evidence from $H_2{}^{18}O/H_2{}^{16}O$. J Geophys Res, 104(C8): 18241-18255, doi:10.1029/1999jc900155.

Kodaira T, Horikawa K, Zhang J, et al. 2016. Relationship between seawater oxygen isotope ratio and salinity in the Tsushima Current, the Sea of Japan. Geochemistry, 50: 263-277, doi:10.14934/chikyukagaku.50.263.

Koutavas A, Joanides S. 2012. El Niño–Southern Oscillation extrema in the Holocene and Last Glacial Maximum. Paleoceanography, 27(4): PA4208, doi:10.1029/2012PA002378.

Kumar P K, Singh A, Ramesh R. 2018. Controls on $\delta^{18}O$, δD and $\delta^{18}O$-salinity relationship in the northern Indian Ocean. Mar Chem, 207: 55-62, doi:10.1016/j.marchem.2018.10.010.

LeGrande A N, Schmidt G A. 2006. Global gridded data set of the oxygen isotopic composition in seawater. Geophys Res Lett, 33(12): L12604, doi:10.1029/2006gl026011.

Macdonald R W, Carmack E C, McLaughlin F A, et al. 1989. Composition and modification of water masses in the Mackenzie shelf estuary. J Geophys Res, 94(C12): 18057-18070, doi:10.1029/jc094ic12p18057.

Macdonald R W, Carmack E C, McLaughlin F A, et al. 1999. Connections among ice, runoff and atmospheric forcing in the Beaufort Gyre. Geophys Res Lett, 26(15): 2223-2226, doi:10.1029/1999gl900508.

Masson-Delmotte V, Hou S, Ekaykin A, et al. 2008. A review of Antarctic surface snow isotopic composition: observations, atmospheric circulation, and isotopic modeling. J Clim, 21(13): 3359-3387,

doi:10.1175/2007jcli2139.1.

Melling H, Moore R M. 1995. Modification of halocline source waters during freezing on the Beaufort Sea shelf: evidence from oxygen isotopes and dissolved nutrients. Cont Shelf Res, 15(1): 89-113, doi:10.1016/0278-4343(94)P1814-R.

Morison J, Kwok R, Peralta-Ferriz C, et al. 2012. Changing Arctic Ocean freshwater pathways. Nature, 481(7379): 66-70, doi:10.1038/nature 10705.

Pang H, Hou S, Landais A, et al. 2015. Spatial distribution of ^{17}O-excess in surface snow along a traverse from Zhongshan Station to Dome A, East Antarctica. Earth Planet Sci Lett, 414: 126-133, doi:10.1016/j. epsl.2015.01.014.

Parkes S D, McCabe M F, Griffiths A D, et al. 2017. Response of water vapour D-excess to land-atmosphere interactions in a semi-arid environment. Hydrol Earth Syst Sci, 21(1): 533-548, doi:10.5194/ hess-21-533-2017.

Pfahl S, Sodemann H. 2014. What controls deuterium excess in global precipitation? Clim Past, 10(2): 771-781, doi:10.5194/cp-10-771- 2014.

Rohling E J, Bigg G R. 1998. Paleosalinity and δ^{18}O: a critical assessment. J Geophys Res: Oceans, 103(C1): 1307-1318, doi:10.1029/97jc01047.

Rohling E J. 2007. Progress in paleosalinity: overview and presentation of a new approach. Paleoceanography, 22(3): PA3215, doi:10.1029/ 2007pa001437.

Roberts J, Gottschalk J, Skinner L C, et al. 2016. Evolution of South Atlantic density and chemical stratification across the last deglaciation. Proc Natl Acad Sci, 113(3): 514-519, doi:10.1073/pnas. 1511252113.

Rozanski K, Araguás-Araguás L, Gonfiantini R. 1993. Isotopic pattern in modern global precipitation//Swart P K, Lohmann K C, Mckenzie J, et al (Eds). Climate change in continental isotopic records, Volume 78. Washington D. C.: American Geophysical Union, 1-36, doi:10.1029/ gm078p0001.

Singh A, Mohiuddin A, Ramesh R, et al. 2014. Estimating the loss of Himalayan glaciers under global warming using the δ^{18}O-salinity relation in the Bay of Bengal. Environ Sci Technol Lett, 1(5): 249-253, doi:10.1021/ez500076z.

Skrzypek G, Ford D. 2014. Stable isotope analysis of saline water samples on a cavity ring-down spectroscopy instrument. Environ Sci Technol, 48(5): 2827-2834, doi:10.1021/es4049412.

Stabeno P J, Schumacher J D, Ohtani K. 1999. The physical oceanography of the Bering Sea//Loughlin T R, Ohtani K (Eds). Dynamics of the Bering Sea. Fairbanks: University of Alaska Sea Grant, AK-SG-99-03, 1-28.

Sowers T, Bender M. 1995. Climate records covering the last deglaciation. Science, 269(5221): 210-214, doi:10.1126/science.269.5221.210.

Uemura R, Matsui Y, Yoshimura K, et al. 2008. Evidence of deuterium excess in water vapor as an indicator of ocean surface conditions. J Geophys Res, 113(D19): D19114, doi:10.1029/2008jd010209.

Xu X, Werner M, Butzin M, et al. 2012. Water isotope variations in the global ocean model MPI-OM. Geosci Model Dev, 5(3): 809-818.

Zhang J, Letolle R, Martin J M, et al. 1990. Stable oxygen isotope distribution in the Huanghe (Yellow River) and the Changjiang (Yangtze River) estuarine systems. Cont Shelf Res, 10(4): 369-384, doi:10.1016/0278-4343(90)90057-S.